Journal of Ceramic Processing Research. Vol. 17, No. 8, pp. 795~798 (2016)

J O U R N A L O F
Ceramic Processing Research

Electrical properties of cobalt-doped zinc manganite ceramics for infrared detectors

Kyeong-Min Kim[a], Myung-Soo Han[b] and Sung-Gap Lee[a,*]

[a]*Department of Materials Engineering and Convergence Technology, Engineering Research Institute, Gyeongsang National University, Jinju 52828, Korea*

[b]*Micro-Optics Team, Korea Photonics Technology Institute, Gwangju 61007, Korea*

$Zn_{1.10}Co_xMn_{1.90-x}O_4$ ($0 \le x \le 0.25$) specimens were prepared using a conventional solid state reaction method. We investigated the structural and electrical properties with varying amounts of Co for application in IR detectors. All specimens exhibited a very dense microstructure and the average grain size decreased slightly with an increase in the composition ratio of Co ions. The $Zn_{1.10}Co_{0.05}Mn_{1.85}O_4$ specimen shows the highest B-value of 5025 K, and the $Zn_{1.10}Co_{0.25}Mn_{1.65}O_4$ specimen shows the minimum resistivity of 100 kΩ · cm. The responsivity,s noise voltage and detectivity of the $Zn_{1.10}Co_{0.10}Mn_{1.80}O_4$ specimen are 0.03 V/W, 6.36×10^{-5}V and 2.010^4 cmHz$^{1/2}$/W, respectively.

Key words: Zn-Co-Mn oxide, Electrical properties, Resistivity, Responsivity, Detectivity.

Introduction

In general, polycrystalline NTC thermistor materials consisting of a mixture of transition metal oxides possess semiconducting properties. Such electronic materials have been widely used for temperature measurement and detection by using the high sensitivity of electrical resistance to temperature. These materials generally have an AB_2O_4 spinel structure, and the electrical conductivity characteristic varies depending on the kind of cation and the amount distributed in tetrahedral and octahedral sites. In particular, the electrical conductivity of Mn-based transition metal spinel oxide ceramics depends on the hopping process as a result of electron exchange between Mn^{3+} and Mn^{4+} ions at octahedral sites [1].

Zinc cations serve to stabilize the spinel structure against oxidation and enhance the stabilization domain of the spinel structure [2]. This characteristic has been extensively studied for application in high temperature thermistor devices. The $ZnMn_2O_4$ material has a tetragonal structure at ambient temperature, and shows a stable spinel phase in air from room temperature to 1100 ºC [3]. In this study, $Zn_{1.10}Co_xMn_{1.90-x}O_4$ specimens were fabricated using the solid state reaction method and the effects of Co ion substitution on the structural and electrical properties for application in uncooled infrared detectors was investigated.

*Corresponding author:
Tel : +82-55-772-1687
E-mail: lsgap@gnu.ac.kr

Experimental

$Zn_{1.10}Co_xMn_{1.90-x}O_4$ ($0 \le x \le 0.25$) specimens were prepared using the solid state reaction method from high-purity ZnO, Mn_2O_3 and Co_3O_4 powders as starting materials. The raw materials were weighed according to the formula and ball-milled for 24 h using zirconia balls as the milling medium. The mixed powders were calcined at 900 ºC for 2 h, blended with an organic binder, sieved and then uniaxially pressed at 1,000 psi to form disk-shaped samples with a diameter of 12 mm and thickness of 2 mm. These powder compacts were sintered at 1200 ºC for 12 h in air.

The structural properties in accordance with the composition ratio of Co cations were analyzed using X-ray diffraction (XRD) and field-emission scanning electron microscopy (FE-SEM). To measure the electrical properties, Ag electrodes were formed on both sides of the ceramic disks using a screen printing method. Electrical resistance was measured with an electrometer (Keithley 6517A, USA) using a two-probe method in a low-temperature chamber (ESPEC SH-241, USA) from –10 ºC to 60 ºC. Infrared detection properties were measured using a blackbody source at 500 ºC, and chopper frequency and bias voltage were 10 Hz and 3 V, respectively.

Results and Discussion

Fig. 1 shows the DTA-TG analysis results for the $Zn_{1.10}Co_{0.10}Mn_{1.80}O_4$ powder. An exothermic peak and mass loss at approximately 220 ºC are observed, corresponding to combustion of the organic materials entrained during the mixing process. The changes in mass between 280 ºC and 800 ºC are thought to be due to the reversible oxidation and reduction reaction of

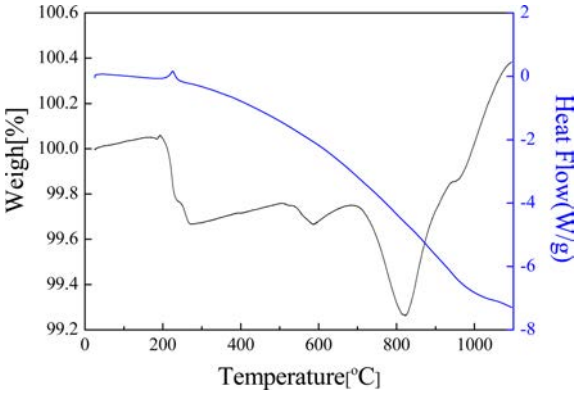

Fig. 1. DTA-TG curves for $Zn_{1.10}Co_{0.10}Mn_{1.80}O_4$ powder.

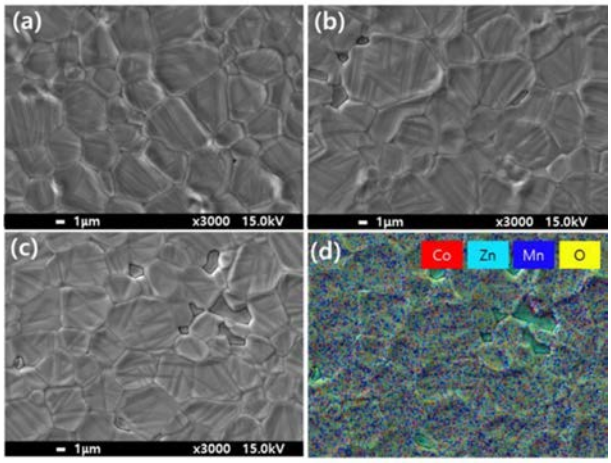

Fig. 2. (a)~(c) FE-SEM surface microstructure image of $Zn_{1.10}Mn_{1.90}O_4$, $Zn_{1.10}Co_{0.05}Mn_{1.85}O_4$, and $Zn_{1.10}Co_{0.10}Mn_{1.80}O_4$ specimens and (d) EDS image of $Zn_{1.10}Co_{0.10}Mn_{1.80}O_4$ specimen.

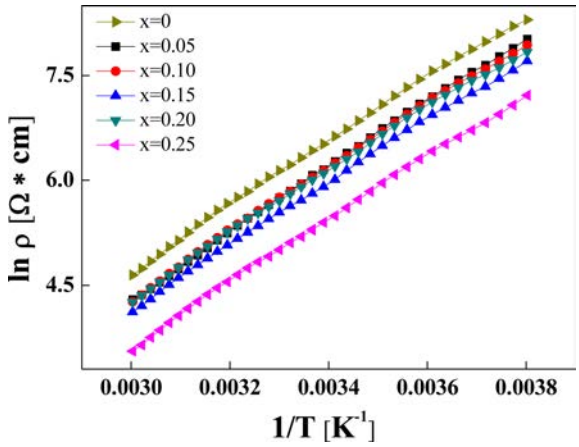

Fig. 3. lnρ vs 1/T plot of $Zn_{1.10}Co_xMn_{1.90-x}O_4$ specimens with varying Co content.

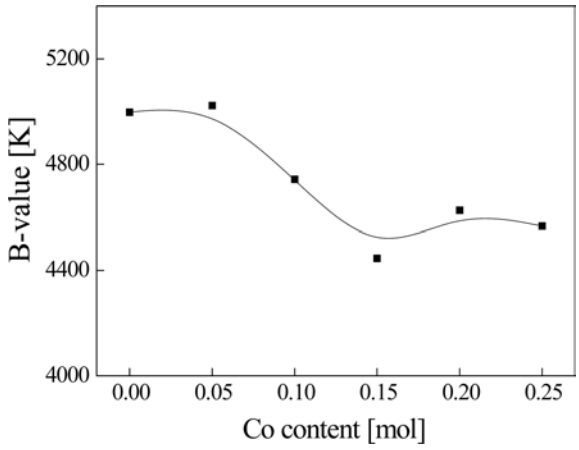

Fig. 4. B-value of $Zn_{1.10}Co_xMn_{1.90-x}O_4$ specimens with varying Co content.

Mn^{4+}/Mn^{3+} ions and the loss of excess oxygen ions [4, 5]. In addition, a continuous mass gain above 800 °C is observed, which corresponds to the formation of the second phase due to ionocovalent bonding between zinc cations and oxygen anions [6, 7]. Generally, the decomposition of Zn-rich zinc manganite spinel phases occurs through the formation of the $ZnMnO_3$ phase [6].

Fig. 2(a) ~ (c) show FE-SEM images of the $Zn_{1.10}Co_xMn_{1.90-x}O_4$ specimens. All specimens exhibited a very dense microstructure and the average grain size decreased slightly with an increase in the composition ratio of Co ions. However, the second phase was observed in the grain boundaries in specimens doped with Co ions ($x \geq 0.05$), and the distribution of the second phase increased with an increase in the amount of Co ions. Fig. 2(d) shows the energy dispersive spectra (EDS) analysis of the $Zn_{1.10}Co_{0.10}Mn_{1.80}O_4$ specimen to observe the distribution of the composition of the second phase. The second phase distributed in the grain boundaries was a Zn-rich Zn-Co-Mn oxide phase, which is thought to be due to the substitution of Zn ions by Co ions in the octahedral sites of the spinel structure.

Fig. 3 shows the relationship between ln ñ and the reciprocal of the absolute temperature. All specimens exhibited typical NTC characteristics where a linear relationship is seen between these two parameters from –10 °C to 60 °C. It presents a good linear relation in the higher temperature zone, i.e. fitting well to the hopping conduction mechanism. However, in the lower temperature zone, the linear characteristic is disturbed and bending occurs as the Co content increases. This can be explained by the fact that the second phase influences the hopping conduction mechanism in manganite-based ceramics in low temperature regions.

Fig. 4 shows the B-value of $Zn_{1.10}Co_xMn_{1.90-x}O_4$ specimens with varying amounts of Co. The coefficient of temperature sensitivity (B-value) can be calculated using $B_{298/323} = \ln(R_{298}/R_{323})/(1/T_{298}-1/T_{323})$, where R_{298} and R_{323} are the resistances measured at 298 K and 323 K, respectively. The B-value decreases with an increase in Co content x, and it tends to be saturated for compositions of $x \geq 0.15$. It can be assumed that, as shown in Fig. 2, the sensitivity characteristics of resistance with variations in temperature decreased as a result of the second phase formed from the addition of Co cations. All

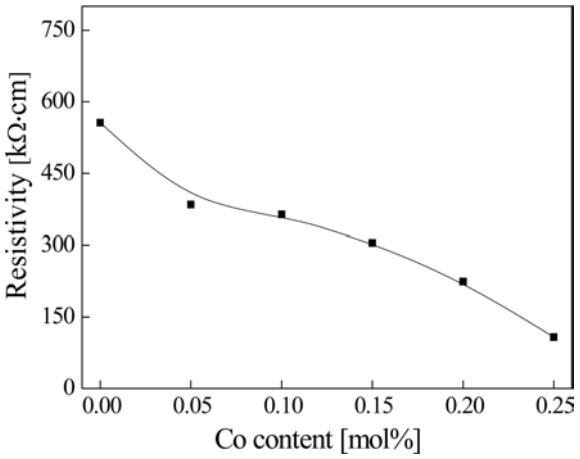

Fig. 5. Resistivity at room temperature of $Zn_{1.10}Co_xMn_{1.90-x}O_4$ specimens with varying Co content.

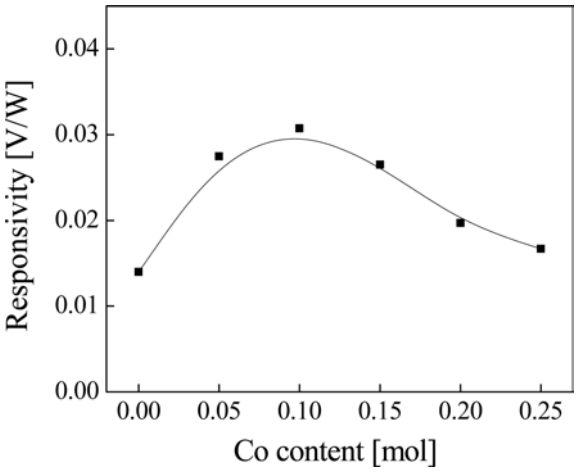

Fig. 6. Responsivity of $Zn_{1.10}Co_xMn_{1.90-x}O_4$ specimens with varying Co content.

specimens display good values higher than 4500 K.

Fig. 5 shows the resistivity at room temperature of $Zn_{1.10}Co_xMn_{1.90-x}O_4$ specimens with varying Co content. The resistivity decreased from 550 kΩ · cm to 100 kΩ · cm with an increase in Co content x from 0 to 0.25. This result suggests that, with an increase in Co content x for $Zn_{1.10}Co_xMn_{1.90-x}O_4$ specimens, Co ions can also occupy octahedral sites in the spinel structure and Mn^{3+}/Mn^{4+} ion pairs are formed in order to maintain the electrical charge neutrality [9].

Fig. 6 shows the responsivity of $Zn_{1.10}Co_xMn_{1.90-x}O_4$ specimens with varying Co content. Responsivity, which indicates the output voltage characteristic for the incident infrared radiation, is affected by the B-value, electrical resistance and thermal conductivity characteristics [10]. In general, responsivity shows an excellent value with a higher B-value and smaller electrical resistivity. The $Zn_{1.10}Co_{0.10}Mn_{1.80}O_4$ specimen exhibited a maximum value of 0.03V/W and then, it tends to decrease as the Co content further increased. This result suggests that for $x \leq 0.10$, the resistivity property has a greater influence on responsivity, and for $x \geq 0.15$, the B-value and

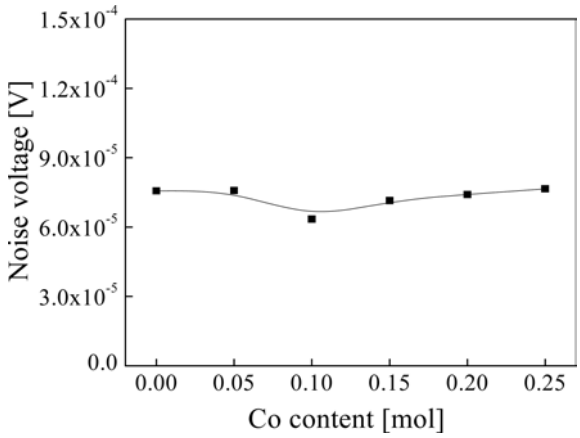

Fig. 7. Noise voltage of $Zn_{1.10}Co_xMn_{1.90-x}O_4$ specimens with varying Co content.

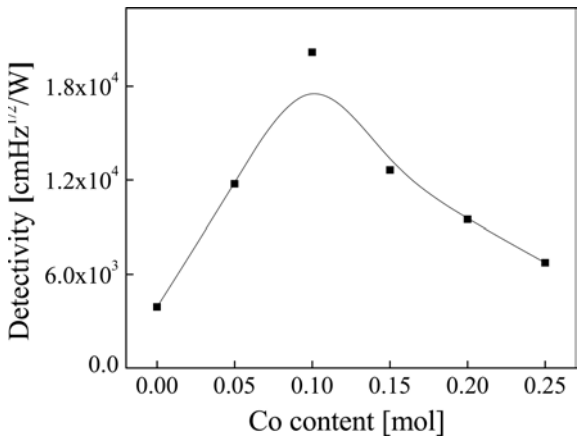

Fig. 8. Detectivity of $Zn_{1.10}Co_xMn_{1.90-x}O_4$ specimens with varying Co content.

thermal conductance properties due to the large amount of the second phase have a greater influence on it.

Fig. 7 shows the noise voltage of $Zn_{1.10}Co_xMn_{1.90-x}O_4$ specimens with varying Co content. Generally, the noise voltage of bolometer-type IR sensors has been mainly influenced by thermal noise due to structural defects in specimens [10]. Dependence of the noise voltage based on Co content was not observed; all specimens showed noise voltages of $6.3 \times 10^{-5} \sim 7.5 \times 10^{-5}$ V. This could be explained by assuming that, in terms of noise voltage properties, effects due to the formation of Mn^{4+} and Mn^{3+} ions and the second phase with the increase in Co content cancel each other out.

Fig. 8 shows the detectivity of $Zn_{1.10}Co_xMn_{1.90-x}O_4$ specimens with varying Co content. Generally, detectivity is very dependent on the responsivity and noise voltage properties. The $Zn_{1.10}Co_{0.10}Mn_{1.80}O_4$ specimen, which exhibited good responsivity and noise voltage properties, showed the highest value of 2.0×10^4 cmHz$^{1/2}$/W.

Conclusions

In this study, we investigated the electrical properties of $Zn_{1.10}Co_xMn_{1.90-x}O_4$ specimens with varying Co

content for application in bolometer IR detectors. The second phase of the Zn-rich Zn-Co-Mn oxide was observed in the grain boundaries with an increase in the Co content. All specimens showed the typical NTC characteristic where electrical resistance decreases with an increase in temperature and resistivity decreases as the composition ratio of Co ions increases. This is thought to be due to the formation of Mn^{3+}/Mn^{4+} ion pairs, while the added Co ions are located in the octahedral sites of the spinel structure to maintain the electrical charge neutrality. The voltage responsivity shows an excellent value with a higher B-value and smaller electrical resistivity.

Acknowledgments

This work was supported by the Industrial Strategic Technology Development Program (No. 10045177, Development of Resistive Ceramic Thin Film using Solution Process and Low Temperature Thin Film Vacuum Getter).

References

1. E. Jabry, G. Boissier, A. Rousset, R. Carnet and A.. Lagrange, J. Phys. Colloque. 47 Suppl.2, (1986) C1-843.
2. S. Guillemet-Fritsch, J.L. Baudour, C. Chanel, F. Bouree, A. Rousset, Solid State Ionics 132 (2000) 63.
3. F.C.M. Driessens, G.D. Rieck, J. Inorg. Nucl. Chem. 28 (1966) 1593.
4. J. Jung, J. Torfer, J. Murbe, A. Feltz, J. Eur. Ceram. Soc. 6 (1990) 351.
5. H.J. Van Daal, A.J. Bosman, Phys. Rev. 158 (1967) 736.
6. S. Guillemet-Fritsch, C. Chanel, J. Sarrias, S. Bayonne, A. Rousset, X. Alcobe, M.L. Martinez Sarrion, Solid State Ionics 128 (2000) 233.
7. D. Fang, Z. Wang, P. Yang, W. Liu and C. Chen, J. Am. Ceram. Soc. 89 (2006) 230.
8. J.L. Martin De Vidales, P. Garcia-Chain, R.M. Rojas, E. Vila, O. Garcia-Martinez, J. Mater. Sci. 33 (1998) 1491.
9. M.N. Muralidharan, P.R. Rohini, E.K. Sunny, K.R. Dayas, A. Seema, Ceramics International, 38 (2012) 6481.
10. E.L. Dereniak and D.G. Crowe, “Optical radiation detectors”, John Wiley & Sons (1984).